Title
A distinct innate lymphoid cell population regulates tumor-associated T cells

Journal
Nature Medicine, 23(3)

ISSN
1078-8956

Authors
Crome, Sarah Q
Nguyen, Linh T
Lopez-Verges, Sandra
et al.

Publication Date
2017-03-01

DOI
10.1038/nm.4278

Peer reviewed

nature medicine

A distinct innate lymphoid cell population regulates tumor-associated T cells

Sarah Q Crome[1], Linh T Nguyen[1], Sandra Lopez-Verges[2,3], S Y Cindy Yang[1,4], Bernard Martin[1], Jennifer Y Yam[1], Dylan J Johnson[1,4], Jessica Nie[1], Michael Pniak[1], Pei Hua Yen[1], Anca Milea[1], Ramlogan Sowamber[1], Sarah Rachel Katz[5], Marcus Q Bernardini[5], Blaise A Clarke[6], Patricia A Shaw[1,6], Philipp A Lang[1,7], Hal K Berman[1,6], Trevor J Pugh[4], Lewis L Lanier[2] & Pamela S Ohashi[1,4]

Antitumor T cells are subject to multiple mechanisms of negative regulation[1–3]. Recent findings that innate lymphoid cells (ILCs) regulate adaptive T cell responses[4–6] led us to examine the regulatory potential of ILCs in the context of cancer. We identified a unique ILC population that inhibits tumor-infiltrating lymphocytes (TILs) from high-grade serous tumors, defined their suppressive capacity *in vitro*, and performed a comprehensive analysis of their phenotype. Notably, the presence of this CD56$^+$CD3$^-$ population in TIL cultures was associated with reduced T cell numbers, and further functional studies demonstrated that this population suppressed TIL expansion and altered TIL cytokine production. Transcriptome analysis and phenotypic characterization determined that regulatory CD56$^+$CD3$^-$ cells exhibit low cytotoxic activity, produce IL-22, and have an expression profile that overlaps with those of natural killer (NK) cells and other ILCs. NKp46 was highly expressed by these cells, and addition of anti-NKp46 antibodies to TIL cultures abrogated the ability of these regulatory ILCs to suppress T cell expansion. Notably, the presence of these regulatory ILCs in TIL cultures corresponded with a striking reduction in the time to disease recurrence. These studies demonstrate that a previously uncharacterized ILC population regulates the activity and expansion of tumor-associated T cells.

ILCs have been classified into three groups with diverse phenotypes and functions[7]. Group 1 includes both cytotoxic NK cells and ILC1s, which also produce interferon (IFN)-γ but are not cytotoxic. Group 2 (ILC2) cells produce IL-4, IL-5, IL-9, and IL-13, and group 3 (ILC3) cells produce IL-22 alone or in combination with IL-17A. These definitions have been complicated by recent studies demonstrating that ILC3 cells can acquire an ILC1-like phenotype (ex-ILC3), that ILC1s exhibit cytotoxicity under certain conditions, and that markers previously used to differentiate ILC populations are often specific to particular immune contexts or tissues[8]. Therefore, the properties that differentiate ILC populations are still poorly understood, particularly in humans.

A dynamic relationship of NK cells and other ILCs with T cells has been described[4,5]. Importantly, in addition to promoting T cell responses, NK cells can inhibit T cell–mediated immune responses in a variety of contexts, including autoimmunity[9–12], transplantation[13,14], and viral infection[15–21]. The significance of NK cell–mediated regulation of T cells has recently been highlighted by mouse studies demonstrating that *in vivo* depletion of NK cells can improve antiviral T cell responses and result in the clearance of lymphocytic choriomeningitis virus (LCMV) clone 13, which normally establishes a chronic infection[19,20]. In humans, NK cells from patients with chronic hepatitis B virus (HBV) infection can kill HBV-specific CD8$^+$ T cells in a TRAIL-receptor-dependent manner[22], and type I interferon treatment of hepatitis C virus (HCV)-infected patients can lead to activation of NK cells and reduced production of IFN-γ by CD4$^+$ T cells[23]. Other reports link activated ILCs with a reduced susceptibility to graft-versus-host disease[24], and ILC3s were shown to limit CD4$^+$ T cell responses to intestinal, commensal bacteria[25], thus supporting a role for non–NK cell ILCs in regulating adaptive responses.

While evaluating the potential of TIL-based adoptive T cell therapy to treat ovarian cancer, we observed a correlation between the presence of CD56$^+$CD3$^-$ cells and poor TIL expansion. TIL cultures from primary high-grade serous cancer (HGSC) were grown using established protocols[26], and the expansion rates and phenotype of the cells present within TIL cultures were assessed (**Fig. 1a–e** and **Supplementary Fig. 1**). A considerable proportion of HGSC TIL cultures grew slowly or failed to expand (**Fig. 1a**) and would therefore not meet criteria for use in adoptive cell therapy. TIL cultures that grew slowly generally corresponded to cultures with a high proportion of CD56$^+$CD3$^-$ cells (**Fig. 1b**,**c**), whereas no association with growth rate was observed for CD14$^+$ or CD19$^+$ populations in TIL cultures (**Fig. 1d**). Further analysis demonstrated that a high proportion of

[1]Princess Margaret Cancer Centre, University Health Network, Toronto, Ontario, Canada. [2]Department of Microbiology and Immunology and the Parker Institute for Cancer Immunotherapy, University of California San Francisco, San Francisco, California, USA. [3]Gorgas Memorial Institute of Health Studies, Panama City, Panama. [4]Departments of Medical Biophysics and Immunology, University of Toronto, Toronto, Ontario, Canada. [5]Division of Gynecologic Oncology, University Health Network, Toronto, Ontario, Canada. [6]Department of Laboratory Medicine and Pathobiology, University of Toronto, Toronto, Ontario, Canada. [7]Department of Molecular Medicine II, Medical Faculty, Heinrich Heine University, Düsseldorf, Germany. Correspondence should be addressed to P.S.O. (pohashi@uhnresearch.ca).

Received 30 September 2016; accepted 4 January 2017; published online 6 February 2017; doi:10.1038/nm.4278

$CD56^+CD3^-$ cells was associated with a reduction in the proportion of $CD4^+$ TILs and, to a greater degree, the proportion of $CD8^+$ TILs (**Fig. 1e**). Both rapidly growing TIL cultures and those that grew slowly or showed no expansion (slow/no expansion) exhibited a range in the proportion of $CD56^+CD3^-$ cells and the proportion of $CD56^+CD3^-$ cells did not have a linear correlation with expansion rate, suggesting that $CD56^+CD3^-$ cells in TIL cultures with slow/no expansion differ from $CD56^+CD3^-$ cells in rapidly expanding cultures in their function.

To address the possibility that some patients had suppressive $CD56^+CD3^-$ cells, TIL cultures with slow/no expansion were cultured with and without depletion of $CD56^+CD3^-$ cells and with irradiated feeder cells, anti-CD3 monoclonal antibody (mAb), and IL-2. This protocol is similar to ones used to rapidly expand TIL cultures immediately before cell infusion in clinical trials. TIL expansion increased in the absence of $CD56^+CD3^-$ cells (**Fig. 1f**). In the majority of patients, an increase in $CD4^+$ and $CD8^+$ TIL expansion was observed in the absence of $CD56^+CD3^-$ cells, but a statistically significant increase in the expansion was noted only for $CD8^+$ TILs (**Fig. 1g**).

To examine whether these $CD56^+CD3^-$ cells could suppress T cells that received a 'strong' proliferative signal and evaluate whether suppression was linked to the presence of antigen-presenting cells (APCs) or IL-2, we performed assays similar to *in vitro* regulatory T cell (T_{reg}) suppression assays. TIL cultures that did not expand well were depleted of $CD56^+CD3^-$ cells and then activated with anti-CD3- and anti-CD28-coated beads. $CD56^+CD3^-$ cells were then added back at a ratio of one $CD56^+CD3^-$ cell to four T cells. The addition of $CD56^+CD3^-$ cells suppressed $CD4^+$ and $CD8^+$ TIL expansion in the absence of APCs or exogenous IL-2 (**Fig. 1h** and **Supplementary Fig. 2**), indicating that $CD56^+CD3^-$ cells from cultures with limited TIL expansion were capable of directly suppressing T cell proliferation. This capacity to inhibit T cell expansion was not shared by $CD56^+CD3^-$ cells from rapidly expanding TIL cultures or when peripheral blood (PB) NK cells were co-cultured with autologous PB T cells (**Supplementary Fig. 3a**,**b**), supporting the interpretation that $CD56^+CD3^-$ cells from slowly expanding TIL cultures represent a distinct regulatory population.

NK cells and other ILCs can contribute to the initiation and polarization of the adaptive immune response[4,5]; therefore, experiments were done to evaluate cytokine production in TIL cultures with slow/no expansion versus those that expanded well. TIL cultures that exhibited slow/no expansion and also contained a high proportion of $CD56^+CD3^-$ cells had lower amounts of IFN-γ, tumor necrosis factor (TNF)-α, IL-4, IL-5, IL-10, and IL-13 but higher amounts of IL-6 (**Fig. 2a**). To determine whether $CD56^+CD3^-$ cells from TIL cultures with slow/no expansion directly regulated TIL cytokine production, sorted $CD56^+CD3^-$ cells were co-cultured with autologous $CD3^+CD56^-$ TILs and activated with anti-CD3- and anti-CD28-coated beads. The percentages of $CD4^+$ and $CD8^+$ TILs that were $TNF\text{-}\alpha^+IFN\text{-}\gamma^+$ were lower in the presence of $CD56^+CD3^-$ cells (**Fig. 2b–d**). Therefore, $CD56^+CD3^-$ cells from cultures with slow/no expansion can directly alter cytokine production by $CD4^+$ and $CD8^+$ TILs.

To interrogate unique and overlapping properties for suppressive $CD56^+CD3^-$ cells from TIL cultures undergoing slow/no expansion (regulatory $CD56^+CD3^-$ cells) and non-suppressive $CD56^+CD3^-$ cells from rapidly expanding TIL cultures ($CD56^+CD3^-$ cells), we performed transcriptome profiling of these populations from six independent donors using RNA–seq (**Fig. 3a–d** and **Supplementary Fig. 4**). Comparison of the fold change in gene-level expression for the two $CD56^+CD3^-$ cell populations revealed a set of significantly differentially expressed genes that distinguished regulatory $CD56^+CD3^-$ cells from nonregulatory $CD56^+CD3^-$ cells, confirming the idea that these two populations are distinct from one another (**Fig. 3a**). The transcriptome profiles of regulatory $CD56^+CD3^-$ cells from three independent donors were remarkably similar, supporting a unique but shared pattern of gene expression among different individuals. When expression of NK cell– and ILC-associated molecules was examined, both populations of $CD56^+CD3^-$ cells had high transcript-level expression of NK cell–associated genes, including natural cytotoxicity receptors (NCRs), members of the NKG2–CD94 family, and killer cell Ig-like receptors (KIRs) (**Fig. 3b**,**c**). High expression of *NCR1* (NKp46), *NCR3* (NKp30), *KLRK1* (NKG2D), *KLRC1* (NKG2A), *KLRD1* (CD94), KIR genes, and *CD7* and low *FCGR3A* (CD16) expression were confirmed by flow cytometry (**Supplementary Figs. 5** and **6**). Regulatory $CD56^+CD3^-$ cells also had high expression of *ID2*, *ZBTB16* (PLZF), *KLRB1* (CD161), *RUNX3*, *TOX*, and *KIT* (CD117) and either low or no detectible expression of *SELL* (CD62L), *B3GAT1* (CD57), and *ITGA2* (CD49b). Interestingly, regulatory $CD56^+CD3^-$ and nonregulatory $CD56^+CD3^-$ populations exhibited high transcript-level expression of *EOMES*, *TBX21*, *GATA3*, *RORA*, and *AHR*, demonstrating a transcription factor expression profile that overlaps with those of NK cells, ILC2s, and ILC3s[27] (**Fig. 3d**). While the regulatory $CD56^+CD3^-$ population was able to suppress antitumor T cells, *FOXP3* could not be detected at either the transcript or protein level (**Fig. 3d** and **Supplementary Fig. 7**), indicating that this T_{reg}-lineage-defining transcription factor[28–30] is not required for ILC-mediated suppression.

To examine cytokine production by the regulatory $CD56^+CD3^-$ population, $CD56^+CD3^-$ cells were sorted from TIL cultures that did not expand well and cultured overnight in medium containing IL-2. Regulatory $CD56^+CD3^-$ cells produced minimal IFN-γ, but they secreted high amounts of IL-9 and IL-22 and low amounts of IL-5, IL-13, and IL-17A (**Fig. 3e**). Despite producing cytokines characteristic of ILC2 and ILC3 cells, regulatory $CD56^+CD3^-$ cells produced very high levels of CCL3 (**Supplementary Fig. 8**), which is reportedly expressed by ILC1s but not by ILC3s[31].

Cytokine expression was further assessed by intracellular cytokine staining. Sorted $CD56^+CD3^-$ cells were restimulated with phorbol myristate acetate (PMA) and ionomycin for 5–6 h. TNF-α and IFN-γ expression could be induced in the ILC populations; however, the two ILC populations differed in the proportions of cells that expressed TNF-α alone, IFN-γ alone, or both TNF-α and IFN-γ (**Fig. 3f**,**g**). Stimulated regulatory $CD56^+CD3^-$ cells produced IL-22, whereas nonregulatory $CD56^+CD3^-$ cells did not, supporting the notion that expression of this cytokine may be a characteristic of regulatory $CD56^+CD3^-$ cells (**Fig. 3h**,**i**). Yet, when analyzed *ex vivo*, regulatory $CD56^+CD3^-$ cells were $NKp44^-$ (**Supplementary Fig. 6c**), distinguishing them from ILC3s[7]. Low IL-9 expression was detected by regulatory $CD56^+CD3^-$ cells in three of five donors, but neither regulatory $CD56^+CD3^-$ nor nonregulatory $CD56^+CD3^-$ cells produced detectable IL-17A under these conditions (**Fig. 3h**). Therefore, this regulatory $CD56^+CD3^-$ population expresses many NK cell–associated receptors but clearly has unique features, including a gene expression signature that distinguishes these cells from nonsuppressive $CD56^+CD3^-$ cells and a unique cytokine and chemokine profile in relation to that of other described ILCs.

A variety of mechanisms have been reported that govern NK cell–mediated T cell regulation. An IL-2- and contact-dependent mechanism was reported in NK cell regulation of T cell responses to human parainfluenza virus type 3 infection[31]. Other studies have observed IL-10-mediated suppression, indirect suppression mediated

by dendritic cells (DCs), and suppression via receptors including 2B4, NKG2D, and NKp46 (refs. 17,19–21). RNA–seq analysis showed that there were high levels of transcripts associated with cytotoxicity, including for granzyme A, granzyme B, and perforin, in the regulatory $CD56^+CD3^-$ population (**Fig. 4a**). Therefore, we assessed the cytotoxic potential of these cells. $CD56^+CD3^-$ cells

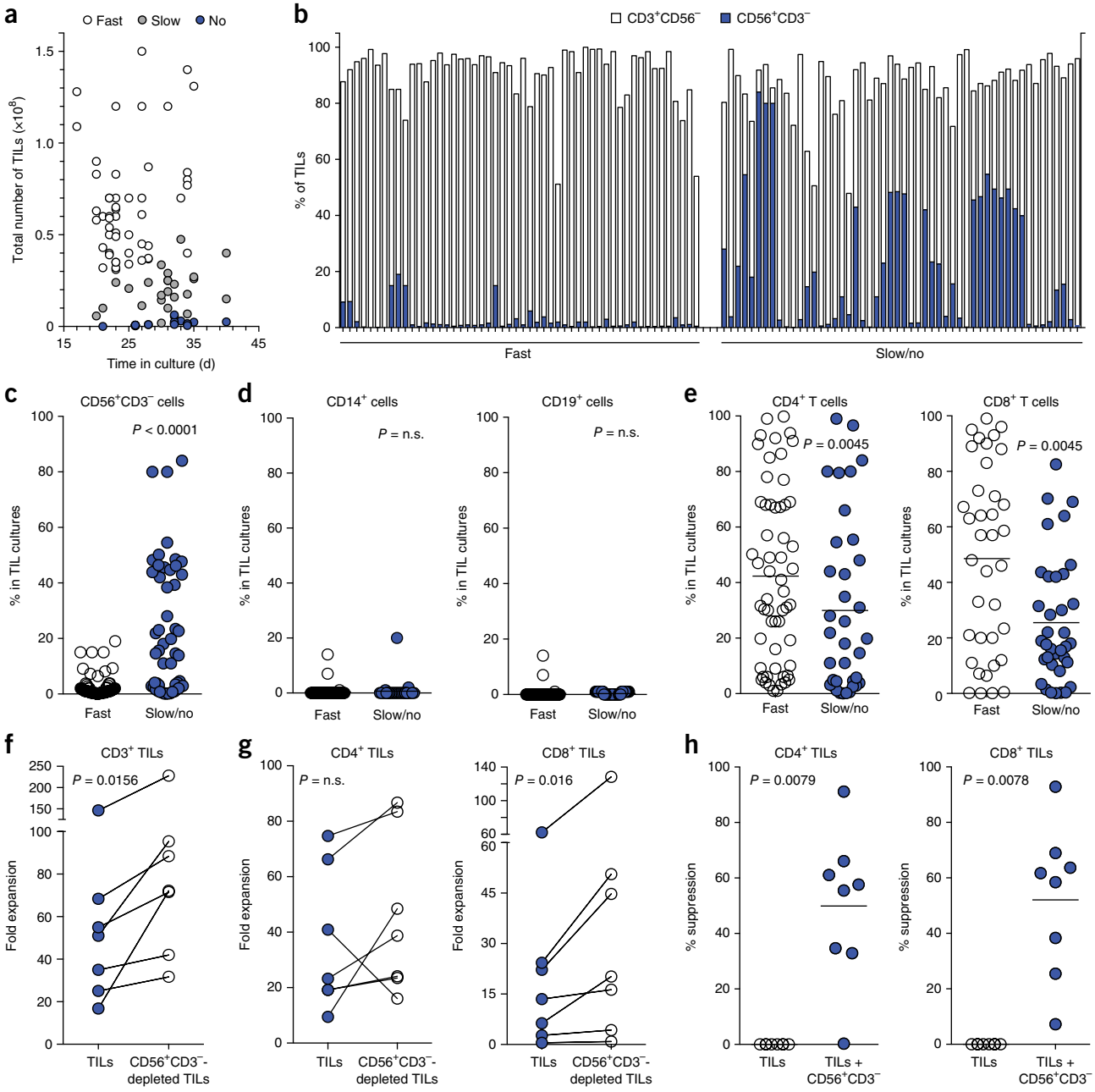

Figure 1 Innate lymphoid cells can suppress the expansion of tumor-infiltrating lymphocytes. (**a**) Multiple TIL cultures from individual HGSC specimens were expanded in medium with IL-2. "Fast" expansion rates refers to TIL cultures that yielded >30 × 10^6 cells on or before 4 weeks in culture, "slow" refers to TIL cultures that yielded 2–29 × 10^6 cells by 4 weeks, and "no" refers to cultures that had cell yields <2 × 10^6 cells at 4 weeks. For cultures that were harvested before or after 4 weeks, the cell counts at the time of harvest were used to estimate whether the culture would have been categorized as "fast", "slow", or "no" at the 4-week mark. (**b**–**e**) Percentages of cells positive for the indicated lineage markers in cultures with fast or slow/no expansion were analyzed. The percentages of cells in TIL cultures are shown for $CD56^+CD3^-$ cells and $CD56^-CD3^+$ cells (fast, $n = 51$; slow/no, $n = 49$) (**b**), $CD56^+CD3^-$ cells (fast, $n = 51$; slow/no, $n = 49$) (**c**), $CD14^+$ cells (fast, $n = 40$; slow/no, $n = 29$) and $CD19^+$ cells (fast, $n = 40$; slow/no, $n = 37$) (**d**), and $CD4^+$ T cells and $CD8^+$ T cells (fast, $n = 37$; slow/no, $n = 36$) (**e**). In **c**–**e**, each circle represents an independent TIL culture. (**f**,**g**) TILs from cultures exhibiting slow/no expansion were stimulated with anti-CD3 antibody, feeder cells, and IL-2 with and without depletion of $CD56^+CD3^-$ cells. Expansion yields were calculated by combining cell counts with flow cytometry analysis of the types of cells present following stimulation. Each circle represents a different patient evaluated ($n = 7$). (**f**) Fold expansion of total $CD3^+$ TILs. (**g**) Fold expansion of $CD4^+$ and $CD8^+$ TILs. (**h**) Flow cytometry–sorted $CD8^+$ and $CD4^+$ TILs from cultures exhibiting slow/no expansion were labeled with cell proliferation dye and activated with anti-CD3 and anti-CD28 antibodies. Expansion in the presence or absence of sorted autologous $CD56^+CD3^-$ cells from TIL cultures experiencing slow/no expansion was assessed at 72 h. Each circle represents a different patient evaluated ($n = 8$). Bars in **c**–**e** and **h** represent the means. Significance was determined by Mann–Whitney test for **c**–**e** and Wilcoxon matched-pairs signed-rank test for **f**–**h**. n.s., not significant.

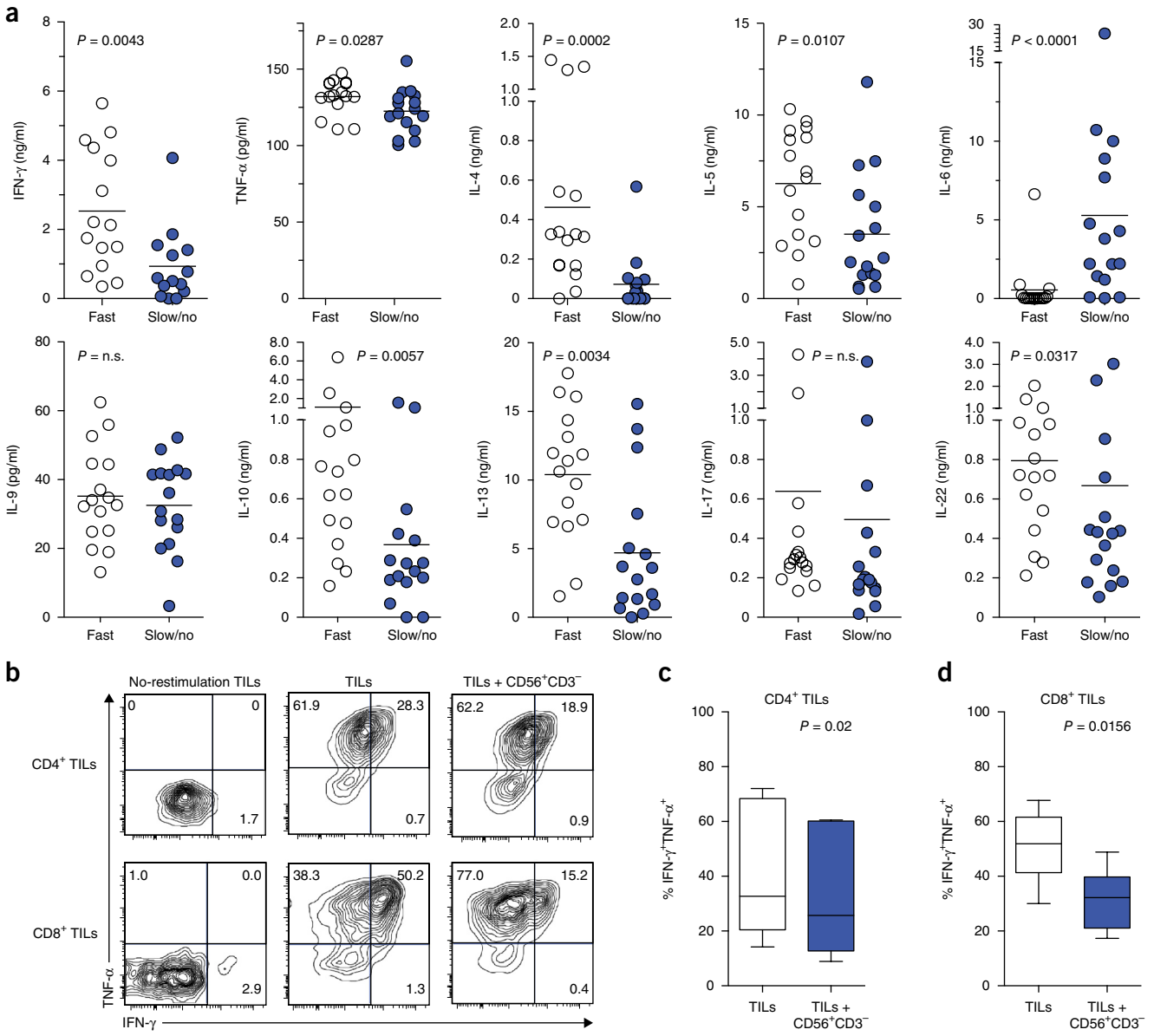

Figure 2 T cell cytokine production is altered in cultures containing regulatory innate lymphoid cells. (**a**) Cytokine production by TIL cultures with slow/no expansion and high proportions of CD56$^+$CD3$^-$ cells and by rapidly expanding TIL cultures with low proportions of CD56$^+$CD3$^-$ cells was assessed by cytometric bead assay. Each circle represents an individual TIL culture from a different patient and bars indicate the mean for each group ($n = 16$). (**b**–**d**) CD8$^+$ and CD4$^+$ TILs from cultures with slow/no expansion sorted by flow cytometry were labeled with cell proliferation dye and activated with anti-CD3 and anti-CD28 antibodies in the presence or absence of sorted autologous CD56$^+$CD3$^-$ cells. Intracellular cytokine production was assessed at 72 h. Representative (**b**) and average CD4$^+$ (**c**) and CD8$^+$ (**d**) TIL expression of IFN-γ and TNF-α in the presence or absence of CD56$^+$CD3$^-$ cells ($n = 7$ patients). For box-and-whisker plots in **c** and **d**, the middle line indicates the median, the box extends from the 25th to 75th percentile, and whiskers indicate minimum to maximum values. Statistical significance was determined by Mann–Whitney test for **a** and by Wilcoxon matched-pairs signed-rank test for **c** and **d**. n.s., not significant.

were sorted from TIL cultures that expanded slowly and were co-cultured with target K562 cells in the presence of IL-2. Regulatory CD56$^+$CD3$^-$ cells had low CD107a expression after co-culture and induced minimal K562 cell death (**Fig. 4b–d**). In comparison, PB NK cells expressed high levels of CD107a and demonstrated strong cytotoxicity against K562 cells.

IL-10 expression by regulatory CD56$^+$CD3$^-$ cells was not observed at either the transcript or protein level (**Fig. 3e** and **Supplementary Fig. 9a**), and there was no increase in *TGFB1* transcript levels when compared to nonregulatory CD56$^+$CD3$^-$ cells (**Supplementary Fig. 9b**). The unique cytokine expression profile of regulatory CD56$^+$CD3$^-$ cells, however, suggested that regulatory CD56$^+$CD3$^-$ cells might suppress T cells via a secreted factor. To address this possibility, CD56$^+$CD3$^-$ cells from TIL cultures with slow/no expansion were sorted by flow cytometry and plated; then, supernatants were collected at 16 h. The expansion and cytokine production of autologous flow cytometry–sorted CD56$^-$CD3$^+$ TILs was then assessed after incubation with and without the supernatants from regulatory CD56$^+$CD3$^-$ cells. No difference in either proliferation or cytokine production was observed (**Fig. 4e,f**).

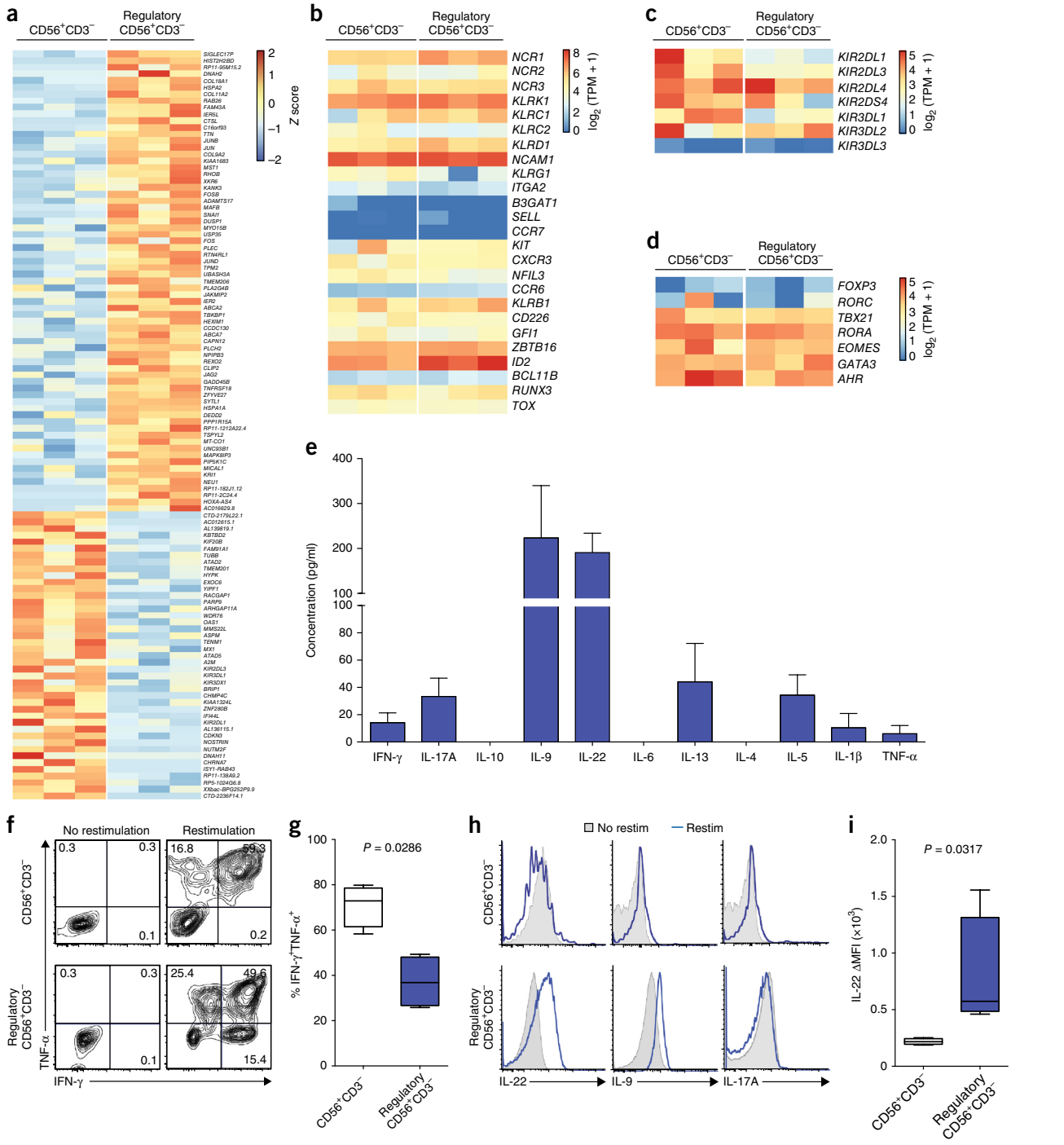

Figure 3 Regulatory innate lymphoid cells have unique properties. RNA–seq was performed on flow cytometry–sorted CD56$^+$CD3$^-$ cells in TIL cultures with slow/no expansion that suppressed TILs (regulatory CD56$^+$CD3$^-$ cells) or CD56$^+$CD3$^-$ cells from TIL cultures with fast expansion that did not suppress TILs (CD56$^+$CD3$^-$ cells). (**a**) Heat map representation of statistically significant differences in gene expression between CD56$^+$CD3$^-$ cells and regulatory CD56$^+$CD3$^-$ cells. The color scale represents the per-gene Z score , which is the number of s.d. away from the mean gene expression value across all samples. Genes were selected on the basis of multiple-testing-adjusted $P < 0.05$ and $\log_2$ (fold change) > 1. (**b**–**d**) Heat map representations of expression of NK cell– and ILC-related molecules (**b**), KIRs (**c**), and transcription factors (**d**) by regulatory CD56$^+$CD3$^-$ cells and CD56$^+$CD3$^-$ cells. The color scale represents log-transformed transcript abundance normalized by the upper quartile measured in transcripts per million (TPM). (**e**) Regulatory CD56$^+$CD3$^-$ cells sorted by flow cytometry were stimulated with IL-2, and supernatants were collected after 24 h. Cytokine expression was measured by cytometric bead assay ($n = 6$ patients). Data are presented as means ± s.e.m. (**f**–**i**) Intracellular cytokine production by regulatory CD56$^+$CD3$^-$ cells and CD56$^+$CD3$^-$ cells sorted by flow cytometry was assessed after 16 h of stimulation with IL-2 and restimulation with PMA and ionomycin. Representative (**f**) and average (**g**) production of TNF-α and IFN-γ by regulatory CD56$^+$CD3$^-$ cells ($n = 4$ patients) and CD56$^+$CD3$^-$ cells ($n = 4$ patients). Representative expression of IL-22, IL-9, and IL-17A (**h**) and average mean fluorescence intensity (MFI) of IL-22 (**i**) by regulatory CD56$^+$CD3$^-$ cells ($n = 5$ patients) and CD56$^+$CD3$^-$ cells ($n = 4$ patients). For box-and-whisker plots in **g** and **i**, the middle line indicates median, the box extends from the 25th to 75th percentile, and whiskers indicate minimum to maximum values. Statistical significance in **g** and **i** was determined by Mann–Whitney test.

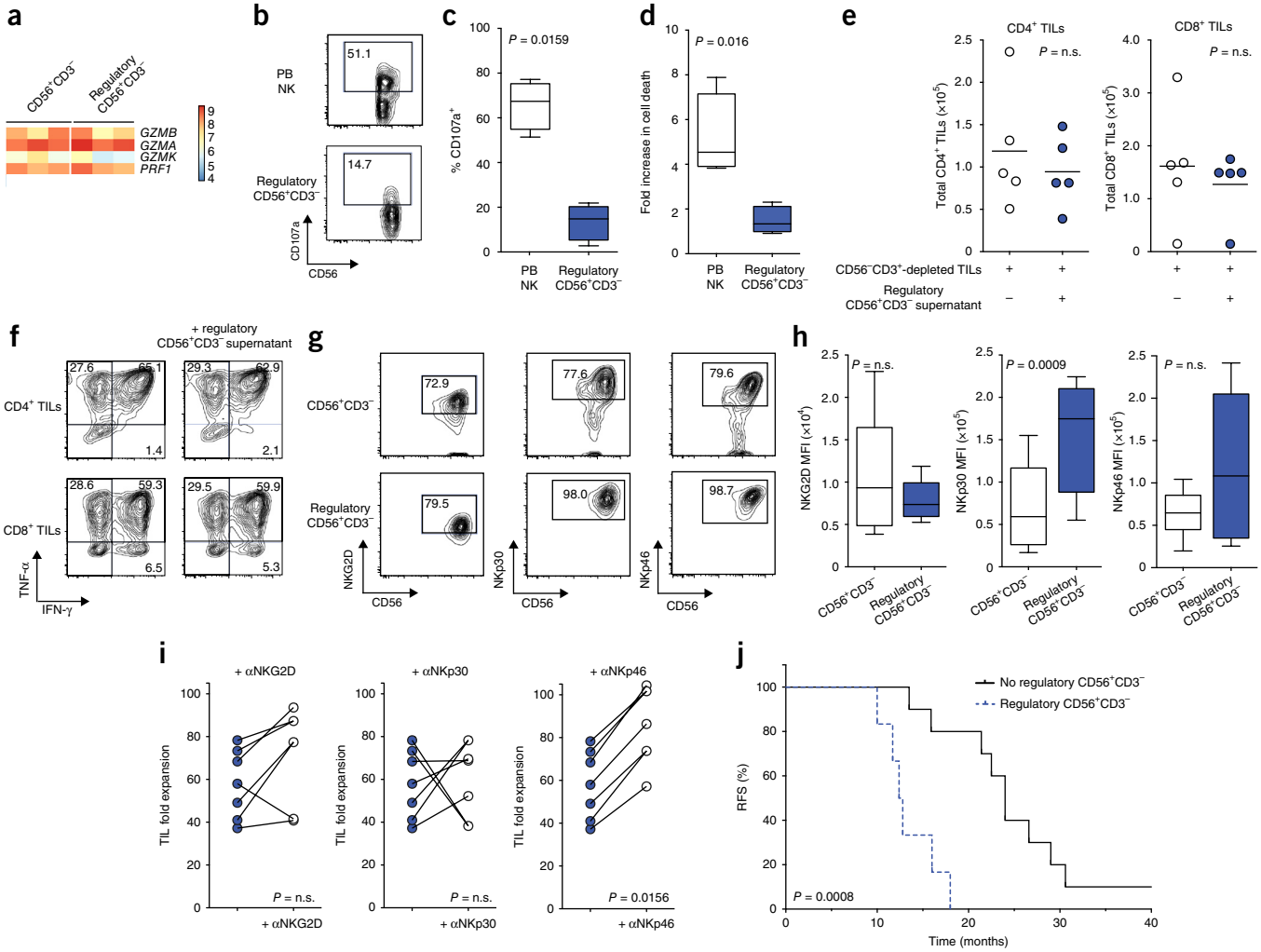

Figure 4 Regulatory innate lymphoid cells limit T cell expansion via natural cytotoxicity receptors, and their presence is associated with a faster time to recurrence. (**a**) Heat map representation of expression of granzymes and perforin on flow cytometry–sorted CD56$^+$CD3$^-$ cells from TIL cultures with slow/no expansion that suppressed TILs (regulatory CD56$^+$CD3$^-$ cells) and CD56$^+$CD3$^-$ cells from TIL cultures with fast expansion that did not suppress TILs (CD56$^+$CD3$^-$ cells). The color scale represents log-transformed transcript abundance normalized to the upper quartile measured in TPM. (**b**–**d**) Regulatory CD56$^+$CD3$^-$ cells and PB NK cells from healthy donors (PB NK) were isolated by flow cytometry–based sorting and co-cultured with K562 cells in the presence of IL-2. CD107a expression by CD56$^+$CD3$^-$ cells and cell death of K562 cells were analyzed after 6 h. Representative (**b**) and average (**c**) CD107a expression by regulatory CD56$^+$CD3$^-$ cells ($n = 5$ patients) or PB NK cells ($n = 4$ healthy donors). (**d**) Average percentage of K562 cells positive for viability dye represented as the fold increase in cell death when K562 cells were co-cultured with regulatory CD56$^+$CD3$^-$ cells ($n = 5$ patients) or PB NK cells ($n = 4$ healthy donors). (**e**,**f**) TIL expansion and cytokine production were analyzed in the presence of supernatants obtained from culturing regulatory CD56$^+$CD3$^-$ cells sorted by flow cytometry. (**e**) The number of CD4$^+$ and CD8$^+$ TILs is shown after expansion with and without supernatants from regulatory CD56$^+$CD3$^-$ cells. Each circle represents a TIL culture from a different patient and the bars represent the means. ($n = 5$). (**f**) Representative intracellular IFN-γ and TNF-α production in CD4$^+$ and CD8$^+$ TILs expanded in the presence or absence of supernatants from regulatory CD56$^+$CD3$^-$ cells for 5 d ($n = 4$). (**g**,**h**) Representative expression (**g**) and mean fluorescence intensity (MFI) average (**h**) of NKG2D, NKp30, and NKp46 expression by regulatory CD56$^+$CD3$^-$ cells and CD56$^+$CD3$^-$ cells from independent TIL cultures ($n = 16$). (**i**) Expansion yields of TILs in the presence or absence of anti-NKG2D, anti-NKp30, or anti-NKp46 antibody were compared following stimulation with feeder cells, anti-CD3 antibody, and IL-2. Each circle represents expansion cultures from a different patient ($n = 7$). (**j**) RFS was analyzed in patients with HGSC whose TIL cultures contained ($n = 6$) or did not contain ($n = 10$) regulatory CD56$^+$CD3$^-$ cells. Patients were chemotherapy naive at the time of TIL isolation, and surgery achieved optimal debulking. For box-and-whisker plots in **c**, **d**, and **h**, the middle line indicates the median, the box extends from 25th to 75th percentile, and the whiskers indicated minimum to maximum values. Statistical significance was determined by Mann–Whitney test for **c**, **d**, **g** and **h**, Wilcoxon matched-pairs signed-rank test for **e** and **i**, and log-rank (Mantel–Cox) test in **j**. n.s., not significant.

Regulatory CD56$^+$CD3$^-$ cells had high expression at the transcript and protein levels of NKG2D (*KLRK1*), as well as NKp30 (*NCR3*) and NKp46 (*NCR1*) (**Fig. 4g**,**h**), two NCRs implicated in the interaction between NK cells and other immune cells[21,32,33]. Therefore, we examined whether these receptors were involved in TIL suppression. TIL cultures with high proportions of CD56$^+$CD3$^-$ cells and slow/no expansion were activated with irradiated feeder cells, anti-CD3 mAb, and IL-2 in the presence or absence of anti-NKG2D, anti-NKp30, and anti-NKp46 antibodies (**Fig. 4i**). Addition of anti-NKG2D antibody to the cultures increased T cell expansion in six of seven patients. As T cells also express NKG2D and anti-NKG2D antibody can be an agonist for T cells, the effects of anti-NKG2D antibody on T cells versus regulatory CD56$^+$CD3$^-$ cells could not be distinguished. However, T cells express neither NKp30 nor NKp46. Addition of anti-NKp30 antibody

increased the expansion yields of T cells in four of seven patients but reduced the yields in two patients. Notably, anti-NKp46 treatment resulted in T cell expansion yields comparable to those achieved by depletion of $CD56^+CD3^-$ cells in all seven patients (**Fig. 1f**), demonstrating that anti-NKp46 treatment interferes with the activity of regulatory $CD56^+CD3^-$ cells. Therefore, the interactions of NKG2D, NKp30, and particularly NKp46 may promote the suppression of TIL expansion that is mediated by regulatory $CD56^+CD3^-$ cells.

The ability of regulatory $CD56^+CD3^-$ cells to suppress autologous TILs suggests that patients with these cells might have reduced immune surveillance. To examine this possibility, we evaluated whether the presence of regulatory $CD56^+CD3^-$ cells in TIL cultures corresponded to a difference in clinical outcomes for patients with HGSC in comparison to patients with fast TIL expansion who did not have a population of regulatory $CD56^+CD3^-$ cells. When recurrence-free survival (RFS) was examined, the average time to recurrence was 12.6 months for patients with regulatory $CD56^+CD3^-$ cells in their TIL cultures versus 24 months for patients who did not have regulatory $CD56^+CD3^-$ cells in their TIL cultures (**Fig. 4j**). The presence of regulatory ILCs in TIL cultures therefore corresponded to a shorter time to relapse. While we did not repeat these studies in an independent cohort, high CD56 expression in the annotated microarray data set published by Tothill *et al.*[34] was associated with a significant reduction in RFS time (**Supplementary Fig. 10**), supporting the interpretation that $CD56^+CD3^-$ cells may be a negative prognostic biomarker for HGSC.

Our findings that some patients with HGSC have TIL cultures containing regulatory $CD56^+CD3^-$ cells while other patients do not suggest that tumor microenvironment may play a role in recruiting and/or promoting the differentiation of immunosuppressive $CD56^+CD3^-$ cells. It is important to note that the association between the presence of $CD56^+CD3^-$ cells and poor TIL expansion is not restricted to HGSC, as we have observed a high proportion of $CD56^+CD3^-$ cells in melanoma and breast cancer TIL cultures that did not expand well (data not shown). In the context of TIL-based adoptive cell therapy, depletion of $CD56^+CD3^-$ cells in expansion protocols may represent a novel method to improve this immunotherapy.

The regulatory $CD56^+CD3^-$ cells that we describe are $CD56^{hi}$ $CD16^-CD94^+NKG2D^+KIR^+NKp30^+NKp46^+$ lymphocytes that can produce IL-22 yet are $NKp44^-$ *ex vivo* and that limit T cell cytokine production and expansion. While capable of making IFN-γ and TNF-α, regulatory $CD56^+CD3^-$ cells do not actively secrete these cytokines in TIL cultures expanded in the presence of IL-2. The majority of cultures contained a high proportion of $CD94^+$ cells and expressed various KIRs, which would point to these cells being of NK cell origin. However, other cultures displayed differences in the expression of NK cell–associated molecules, leaving the possibility of a heterogeneous $CD56^+CD3^-$ ILC population in these individuals. However, our study clearly demonstrates that the ability of regulatory $CD56^+CD3^-$ cells to suppress TILs involves NKp46, supporting a role for this NCR in regulating interactions with T cells.

Notably, ILCs and NK cells with immunosuppressive capacity in our study and others have been found to have many of the same characteristics as T_{reg} cells. In addition to suppressing T cell expansion and cytokine production, some models have shown that suppressive NK cells/ILCs produce IL-10 (refs. 35,36), inhibit B cell function and memory[37,38], and dampen immune responses by modulating DC function[39–41], as well as limiting immunity by killing $CD8^+$ T cells[19,20]. While the majority of studies have described immunosuppressive ILCs as NK cells, the various shared and distinct properties of suppressive ILCs when compared to conventional NK cells and other ILC subsets are not well defined. From this perspective, the origin and differentiation of regulatory ILCs must be better understood. The extent to which ILCs regulate immune responses in a multitude of contexts should be evaluated, as this is important for understanding human disease.

METHODS

Methods, including statements of data availability and any associated accession codes and references, are available in the online version of the paper.

Note: Any Supplementary Information and Source Data files are available in the online version of the paper.

ACKNOWLEDGMENTS

We thank the donors for participating in this study and C. Tran and C. Garcia-Batres for helpful comments. We thank the Princess Margaret Genomics Centre (Toronto, Canada) for performing RNA sequencing. We thank M. Pintiles for her advice regarding statistical analysis of results. S.Q.C. is a Banting Fellow and was supported by a Knudson postdoctoral fellowship. S.L.-V. was supported by a Cancer Research Institute/Irvington Institute postdoctoral fellowship and is now part of Sistema Nacional de Investigación (SNI) de SENACYT, Panamá. T.J.P. is supported by the Princess Margaret Cancer Foundation, the Canada Foundation for Innovation, the Leaders Opportunity Fund (CFI 32383), and the Ontario Ministry of Research and Innovation, Ontario Research Fund Small Infrastructure Program. P.A.L. is supported by the Alexander von Humboldt Foundation (SKA2010) and the German Research Council (LA2558/3-1, LA2558/5-1, SFB974, RTG1949). L.L.L. is an American Cancer Society Professor funded by US National Institutes of Health grants AI066897 and AI068129 and the Parker Institute for Cancer Immunotherapy. P.S.O. holds a Canada Research Chair in Autoimmunity and Tumor Immunity. Canadian Institutes for Health Research grant CCM 104887 and CIHR Foundation award FDN143220 to P.S.O. supported this work.

AUTHOR CONTRIBUTIONS

S.Q.C. and P.S.O. designed and supervised the project, analyzed the data, and wrote the manuscript. L.T.N., S.L.-V. and L.L.L. designed and analyzed experiments. L.T.N., S.L.-V., L.L.L., P.A.L. and D.J.J. also edited the manuscript. S.Y.C.Y. and T.J.P. performed the RNA–seq analysis. B.M. and H.K.B. evaluated outcome data in published microarray data sets. A.M., R.S., B.A.C. and P.A.S. performed immunohistochemistry staining and analysis to confirm HGSC. J.Y.Y., D.J.J., J.N., M.P. and P.H.Y. assisted with experiments. S.R.K., M.Q.B. and P.A.S. collected patient clinical data.

COMPETING FINANCIAL INTERESTS

The authors declare no competing financial interests.

1. Smyth, M.J., Ngiow, S.F., Ribas, A. & Teng, M.W. Combination cancer immunotherapies tailored to the tumour microenvironment. *Nat. Rev. Clin. Oncol.* **13**, 143–158 (2016).
2. Callahan, M.K., Postow, M.A. & Wolchok, J.D. Targeting T cell co-receptors for cancer therapy. *Immunity* **44**, 1069–1078 (2016).
3. Schildberg, F.A., Klein, S.R., Freeman, G.J. & Sharpe, A.H. Coinhibitory pathways in the B7–CD28 ligand–receptor family. *Immunity* **44**, 955–972 (2016).
4. Crome, S.Q., Lang, P.A., Lang, K.S. & Ohashi, P.S. Natural killer cells regulate diverse T cell responses. *Trends Immunol.* **34**, 342–349 (2013).
5. Gasteiger, G. & Rudensky, A.Y. Interactions between innate and adaptive lymphocytes. *Nat. Rev. Immunol.* **14**, 631–639 (2014).
6. Artis, D. & Spits, H. The biology of innate lymphoid cells. *Nature* **517**, 293–301 (2015).
7. Spits, H. *et al.* Innate lymphoid cells—a proposal for uniform nomenclature. *Nat. Rev. Immunol.* **13**, 145–149 (2013).
8. Spits, H., Bernink, J.H. & Lanier, L. NK cells and type 1 innate lymphoid cells: partners in host defense. *Nat. Immunol.* **17**, 758–764 (2016).
9. Takeda, K. & Dennert, G. The development of autoimmunity in C57BL/6 lpr mice correlates with the disappearance of natural killer type 1–positive cells: evidence for their suppressive action on bone marrow stem cell proliferation, B cell immunoglobulin secretion, and autoimmune symptoms. *J. Exp. Med.* **177**, 155–164 (1993).
10. Villanueva, J. *et al.* Natural killer cell dysfunction is a distinguishing feature of systemic onset juvenile rheumatoid arthritis and macrophage activation syndrome. *Arthritis Res. Ther.* **7**, R30–R37 (2005).

11. Zhou, R., Wei, H. & Tian, Z. NK3-like NK cells are involved in protective effect of polyinosinic–polycytidylic acid on type 1 diabetes in nonobese diabetic mice. *J. Immunol.* **178**, 2141–2147 (2007).
12. Tai, L.H. *et al.* Positive regulation of plasmacytoid dendritic cell function via Ly49Q recognition of class I MHC. *J. Exp. Med.* **205**, 3187–3199 (2008).
13. Beilke, J.N., Kuhl, N.R., Van Kaer, L. & Gill, R.G. NK cells promote islet allograft tolerance via a perforin-dependent mechanism. *Nat. Med.* **11**, 1059–1065 (2005).
14. Rivas, M.N. *et al.* NK cell regulation of CD4 T cell–mediated graft-versus-host disease. *J. Immunol.* **184**, 6790–6798 (2010).
15. Su, H.C. *et al.* NK cell functions restrain T cell responses during viral infections. *Eur. J. Immunol.* **31**, 3048–3055 (2001).
16. Noone, C.M. *et al.* Natural killer cells regulate T-cell proliferation during human parainfluenza virus type 3 infection. *J. Virol.* **82**, 9299–9302 (2008).
17. Waggoner, S.N., Taniguchi, R.T., Mathew, P.A., Kumar, V. & Welsh, R.M. Absence of mouse 2B4 promotes NK cell–mediated killing of activated $CD8^+$ T cells, leading to prolonged viral persistence and altered pathogenesis. *J. Clin. Invest.* **120**, 1925–1938 (2010).
18. Soderquest, K. *et al.* Cutting edge: $CD8^+$ T cell priming in the absence of NK cells leads to enhanced memory responses. *J. Immunol.* **186**, 3304–3308 (2011).
19. Waggoner, S.N., Cornberg, M., Selin, L.K. & Welsh, R.M. Natural killer cells act as rheostats modulating antiviral T cells. *Nature* **481**, 394–398 (2011).
20. Lang, P.A. *et al.* Natural killer cell activation enhances immune pathology and promotes chronic infection by limiting $CD8^+$ T-cell immunity. *Proc. Natl. Acad. Sci. USA* **109**, 1210–1215 (2012).
21. Narni-Mancinelli, E. *et al.* Tuning of natural killer cell reactivity by NKp46 and Helios calibrates T cell responses. *Science* **335**, 344–348 (2012).
22. Peppa, D. *et al.* Up-regulation of a death receptor renders antiviral T cells susceptible to NK cell–mediated deletion. *J. Exp. Med.* **210**, 99–114 (2013).
23. Ahlenstiel, G. *et al.* Early changes in natural killer cell function indicate virologic response to interferon therapy for hepatitis C. *Gastroenterology* **141**, 1231–1239.e2 (2011).
24. Munneke, J.M. *et al.* Activated innate lymphoid cells are associated with a reduced susceptibility to graft-versus-host disease. *Blood* **124**, 812–821 (2014).
25. Hepworth, M.R. *et al.* Innate lymphoid cells regulate $CD4^+$ T-cell responses to intestinal commensal bacteria. *Nature* **498**, 113–117 (2013).
26. Nguyen, L.T. *et al.* Expansion and characterization of human melanoma tumor-infiltrating lymphocytes (TILs). *PLoS One* **5**, e13940 (2010).
27. Koues, O.I. *et al.* Distinct gene regulatory pathways for human innate versus adaptive lymphoid cells. *Cell* **165**, 1134–1146 (2016).
28. Hori, S., Nomura, T. & Sakaguchi, S. Control of regulatory T cell development by the transcription factor Foxp3. *Science* **299**, 1057–1061 (2003).
29. Fontenot, J.D., Gavin, M.A. & Rudensky, A.Y. Foxp3 programs the development and function of $CD4^+CD25^+$ regulatory T cells. *Nat. Immunol.* **4**, 330–336 (2003).
30. Khattri, R., Cox, T., Yasayko, S.A. & Ramsdell, F. An essential role for Scurfin in $CD4^+CD25^+$ T regulatory cells. *Nat. Immunol.* **4**, 337–342 (2003).
31. Bernink, J.H. *et al.* Human type 1 innate lymphoid cells accumulate in inflamed mucosal tissues. *Nat. Immunol.* **14**, 221–229 (2013).
32. Roy, S. *et al.* NK cells lyse T regulatory cells that expand in response to an intracellular pathogen. *J. Immunol.* **180**, 1729–1736 (2008).
33. Simhadri, V.R. *et al.* Dendritic cells release HLA-B-associated transcript-3 positive exosomes to regulate natural killer function. *PLoS One* **3**, e3377 (2008).
34. Tothill, R.W. *et al.* Novel molecular subtypes of serous and endometrioid ovarian cancer linked to clinical outcome. *Clin. Cancer Res.* **14**, 5198–5208 (2008).
35. Lee, S.H., Kim, K.S., Fodil-Cornu, N., Vidal, S.M. & Biron, C.A. Activating receptors promote NK cell expansion for maintenance, IL-10 production, and CD8 T cell regulation during viral infection. *J. Exp. Med.* **206**, 2235–2251 (2009).
36. Fodil-Cornu, N. *et al.* Ly49h-deficient C57BL/6 mice: a new mouse cytomegalovirus-susceptible model remains resistant to unrelated pathogens controlled by the NK gene complex. *J. Immunol.* **181**, 6394–6405 (2008).
37. Rydyznski, C.E. & Waggoner, S.N. Boosting vaccine efficacy the natural (killer) way. *Trends Immunol.* **36**, 536–546 (2015).
38. Che, S. & Huston, D.P. Natural killer cell suppression of IgM production. *Nat. Immun.* **13**, 258–269 (1994).
39. Chiesa, M.D. *et al.* The natural killer cell–mediated killing of autologous dendritic cells is confined to a cell subset expressing CD94/NKG2A, but lacking inhibitory killer Ig-like receptors. *Eur. J. Immunol.* **33**, 1657–1666 (2003).
40. Piccioli, D., Sbrana, S., Melandri, E. & Valiante, N.M. Contact-dependent stimulation and inhibition of dendritic cells by natural killer cells. *J. Exp. Med.* **195**, 335–341 (2002).
41. Spaggiari, G.M. *et al.* NK cell–mediated lysis of autologous antigen-presenting cells is triggered by the engagement of the phosphatidylinositol 3-kinase upon ligation of the natural cytotoxicity receptors NKp30 and NKp46. *Eur. J. Immunol.* **31**, 1656–1665 (2001).

ONLINE METHODS

Tissue and blood specimens. This study was conducted according to the principles expressed in the Declaration of Helsinki. The Research Ethics Board (REB) of the University Health Network (UHN) approved the study. All patients provided written informed consent for the collection of samples. Fresh tissues were obtained from patients with ovarian cancer undergoing standard-of-care surgical procedures (UHN REB 10-0335). Tissues were obtained from the UHN Biospecimen Sciences Program. Blood products for TIL growth and assays were obtained from donors with hemochromatosis who were undergoing therapeutic phlebotomy (UHN REB 06-0129).

Phenotypic and functional study restrictions. Functional and phenotypic experiments were performed using tissue from patients with confirmed HGSC and were chemotherapy naive at the time of surgery. Tissues were obtained from initial debulking surgeries. Clinicians providing patient outcome data, diagnosis, and analysis of IHC sections were blinded to TIL expansion rates and the outcomes of functional/phenotypic studies.

Media. The complete medium (CM) for initial TIL expansion was comprised of Iscove's modified Dulbecco's medium (IMDM) (Lonza) with 10% human plasma, 25 mM HEPES (Lonza), 100 U/ml penicillin, 100 μg/ml streptomycin (Lonza), 10 μg/ml gentamicin sulfate (Lonza), 2 mM L-glutamine (Lonza), 5.5×10^{-5} M 2-mercaptoethanol (Invitrogen), and 6,000 IU/ml recombinant human IL-2 (Novartis). For enzyme dissociation medium, the following were added to IMDM: 1 mg/ml collagenase (Sigma), 100 μg/ml DNase I (pulmozyme, Roche), 10 μg/ml gentamicin sulfate, 2 mM L-glutamine, 1.25 μg/ml amphotericin B, 100 U/ml penicillin, and 100 μg/ml streptomycin. XH Media used for suppression assays consisted of X-Vivo 15 (Lonza) plus 5% human plasma, 100 U/ml penicillin, 100 μg/ml streptomycin (Lonza), and 2 mM L-glutamine (Lonza).

Tumor-infiltrating lymphocyte cultures. Methods for the initial TIL expansion are described in Nguyen *et al.*[26]. In brief, tissues were processed by mincing into ~1 mm^3 pieces and plated in 24-well tissue culture plates, or by enzymatic dissociation before plating at 1×10^6 cells per well. Cells were cultured in 2 ml of CM (containing 6,000 IU/ml recombinant human IL-2) per well in a humidified incubator with 5% CO_2 at 37 °C. During culture, half of the medium from each well was replaced with fresh CM three times a week, and wells were maintained at a cell concentration of $0.5–2 \times 10^6$ cells/ml. Each independent TIL culture was generally derived from one parental well; during subsequent expansion, all daughter wells derived from the same parental well were combined, mixed, and replated. "Fast" expansion rates refers to TIL cultures that yielded $>30 \times 10^6$ cells on or before 4 weeks, "slow" refers to TIL cultures that achieved $2–29 \times 10^6$ cells by 4 weeks, and "no" refers to cultures that had cell yields below 2×10^6 cells at 4 weeks. TIL culturing was initially performed to assess whether enough cells could be expanded for adoptive T cell therapy clinical trials. Therefore, these criteria are based on the cell numbers needed within a short (maximum of 4 weeks) timeframe to seed rapid expansion protocols (REPs) in order to generate enough cells for infusion under clinical protocols. For cultures that were harvested before or after 4 weeks, the counts at the time of harvest were used to estimate whether the culture would have been categorized as "fast," "slow," or "no" at the 4-week mark. Therefore, some of the cultures in the "slow" category had $>30 \times 10^6$ cells at the time of harvest (>4 weeks in culture).

Further expansion of TILS after depletion of regulatory ILCs. For all expansion and functional studies, $CD56^+CD3^-$ cells were also $CD14^-$ and $CD19^-$. TIL cultures with a high proportion of $CD56^+CD3^-$ cells and a low expansion rate were thawed, replated at 5×10^6 cells/well, and rested in CM (containing 6,000 IU/ml IL-2) for 7 d. On day 7, TILs were depleted of $CD56^+CD3^-$ cells by flow cytometry–based sorting. Cultures were then subjected to further expansion in CM in 24-well plates as follows: 1×10^4 TILs depleted of $CD56^+CD3^-$ cells or non-sorted TILs, 1×10^6 TM-LCL Epstein–Barr virus (EBV)-transformed B-lymphoblastoid line (LCL) (kind gift from C. Yee (MD Anderson)) irradiated with 7,500 Gy, 5×10^6 allogeneic peripheral blood mononuclear cells (PBMCs) irradiated with 45 Gy, 30 ng/ml anti-CD3 antibody (OKT3, Miltenyi Biotec) and 600 IU/ml IL-2. Fresh CM containing IL-2 was added every 2–3 d. Cell counts were performed every 2–3 d in parallel with flow cytometric analysis of CD3, CD4, CD8, and CD56 expression. Cell counts were multiplied by the percentage of cells that were $CD56^+CD3^-$, $CD4^+$ T cells ($CD3^+CD4^+CD8^-$) or $CD8^+$ T cells ($CD3^+CD4^-CD8^+$) to calculate expansion yields.

Suppression assays. $CD56^+CD3^-$ cells and $CD4^+$ and $CD8^+$ T cells were purified by flow cytometry–based sorting (BD Aria). For all suppression assays, $CD56^+CD3^-$ cells were also $CD14^-$ and $CD19^-$. T cells were labeled with Cell Proliferation Dye (eBioscience) and then stimulated at 1×10^5 cells/well with anti-CD3- and anti-CD28-coated beads (Invitrogen) in the presence or absence of sorted autologous $CD56^+CD3^-$ cells from the slowly expanding TIL cultures (regulatory $CD56^+CD3^-$ cells) at a 1:4 ratio of $CD56^+CD3^-$ cells to T cells. After 72 h, the number of cells present was determined, as was the proportions of cells expressing CD3, CD4, CD8, and CD56. Percentage suppression was calculated using the following formula commonly used to calculate suppression by T_{reg} cells: suppression (%) = (1 – (TILs + $CD56^+CD3^-$ cells/TILs)) × 100%. Cytokine suppression was determined by analysis of intracellular cytokine staining of sorted $CD4^+$ and $CD8^+$ T cells (1×10^5 cells/well) that had been stimulated for 72 h with anti-CD3- and anti-CD28-coated beads (Invitrogen) in the presence or absence of autologous purified regulatory $CD56^+CD3^-$ cells. Cell Stimulation Cocktail (eBioscience) was used to restimulate T cells for 5–6 h, with brefeldin A (eBioscience) added halfway through the restimulation. Following surface staining, cells were fixed using Cytofix/Cytoperm buffer (BD). Intracellular cytokine staining was performed in Cytoperm buffer (BD) with monoclonal antibodies against TNF-α (BD, Mab11, 1:100) and IFN-γ (BD, B27, 1:100). Samples were acquired on a FACSCanto II (BD), and data were analyzed with FlowJo software.

For suppression assays involving supernatants from regulatory $CD56^+CD3^-$ cells, supernatants from sorted $CD56^+CD3^-$ cells were added every day for the duration of the assay and suppression was measured as above.

RNA preparation and RNA sequencing. $CD56^+CD3^-CD19^-CD14^-$ cells from slowly growing TIL cultures that were confirmed to suppress TILs in functional assays (regulatory $CD56^+CD3^-$ cells) and $CD56^+CD3^-CD19^-CD14^-$ cells from rapidly expanding TIL cultures that did not suppress TILs in functional assays ($CD56^+CD3^-$ cells) were sorted by flow cytometry. RNA was isolated using RNeasy Plus Mini kits (Qiagen). RNA preparations were quantified by High-Sensitivity RNA Qubit assay (Life Technologies/Thermo Fisher) and quality by Agilent Bioananlyzer. All samples in this study showed high RNA quality, having RINs between 8.1 and 9.8. 1.5 ng of total RNA per sample was used for library preparation using SMARTer Stranded Total RNA-seq Kit-Pico Input Mammalian (Clontech Laboratories). The paired-end libraries were sequenced on NextSeq 500 (Illumina) for 75 cycles. RNA–seq was performed by the Princess Margaret Genomics Centre (Toronto, Canada)

RNA sequencing data analysis. For each sample, raw sequence files in FASTQ format containing an average of 150 million reads were aligned to the GRCh37 human reference genome using STAR v.2.4.2a assisted by the GENCODE v19 transcriptome model annotations[42]. Data alignment quality control measures were collected and verified using RNA-SeQC v1.1.8 (ref. 43). Because of the limited DNA input used for sequencing, only highly expressed transcripts could be detected with sufficient sequencing read coverage (**Supplementary Fig. 4**). Gene-level transcript abundances were quantified using RSEM v1.2.29 and is reported in units of transcripts per million (TPM)[44]. Gene expression heat maps were created by $\log_2$-transformed, upper-quartile-normalized TPM values using custom scripts in the R statistical environment. The DESeq2 R package was used to perform principal-component analysis and identify differentially expressed genes by using expected read counts generated by RSEM[45]. Differentially expressed genes with *P* values adjusted for multiple testing by FDR less than 0.05 and $\log_2$ fold change greater than 1 are reported as statistically significant.

Flow cytometric analyses. Surface marker staining for the following markers was performed in PBS at 4 °C for 30 min following Fc block:

(CD3 (BD and eBiosciences, UCHT1 or BioLegend, OKT3), CD4 (eBioscience or BD, RPA-T4), CD8 (BD, RPA-T8 or Beckman Coulter, B9.11), CD56 (BD, B159 or BioLegend , HCD56), CD335 (NKp46) (BioLegend, 9E2), NKp44 (CD336) (BD, p44-8.1), NKp30 (CD337) (BioLegend, P30-15), CD16 (BD or BioLegend, 3G8, or eBioscience, eBioCB16(CB16)), CD27 (BioLegend, O323), CD158/KIR2DL5 (eBioscience, clone UP-R1), CD57 (eBioscience, TB01), CD94 (R&D Systems, 131412), NKG2C (CD159c) (R&D Systems, 134591), NKG2A (CD159a) (R&D Systems, 131411), NKG2D (CD159d) (R&D Systems, 149810), KIR3DL1(BD, DX9), KIR2DL3 (R&D Systems, 180701), KIR3DL1/3DS1 (Beckman Coulter, Z27), KIR2DL3/2DS2/2DL2 (Merck Research Labs, DX27), KIR3DL2 (Merck Research Labs, DX31), KIR2DS4 (R&D Systems, 179315), LIR-1 (HP-FI generously provided by M. Lopez-Botet, Universitat Pompeu Fabra), CD7 (BD, M-T701), CD19 (BioLegend, HIB19), CD14 (BioLegend, M5E2), FOXP3 (eBioscience, 236A/E7), and Fixable Viability Dye (eBioscience). Following surface staining, cells were washed and fixed in 2% paraformaldehyde in PBS or BD Cytofix/Cytoperm buffer, depending on the markers analyzed. For intracellular cytokine staining of, $CD56^+CD3^-$ cells, Cell Stimulation Cocktail (eBioscience) was used to restimulate T cells for 5–6 h, with brefeldin A (eBioscience) added 1 h after restimulation. Following surface staining, cells were fixed using Cytofix/Cytoperm buffer (BD). Intracellular cytokine staining was performed in Cytoperm buffer (BD) with monoclonal antibodies against TNF-α (BD, Mab11), IFN-γ (BD, B27), IL-9 (eBioscience, MH9D1), IL-22 (eBioscience, 22URT1), and IL-17A (eBioscience, eBio64DEC17). For the phenotyping and intracellular cytokine staining flow cytometry analyses, $CD56^+CD3^-$ cells were also $CD14^-$ and $CD19^-$. Dilutions of antibodies ranged from 1:10 to 1:200, with the exception of fixable viability dye, which was used at 1:1,000. Dilutions were titrated for each lot, assay, and fluorochrome. Samples were acquired on a FACSCanto II (BD), and data were analyzed with FlowJo software.

Cytokine and chemokine assays. 13-Plex Flow cytomix bead arrays (eBioscience) were used following the manufacturer's instructions to quantify the amounts of cytokines in 24-h supernatants from TIL cultures, which were plated at 1×10^6 cells/ml in 24-well plates with 6,000 IU/ml IL-2 in CM. To quantify secreted cytokines and chemokines, $CD56^+CD3^-CD19^-CD14^-$ cells were plated at a concentration of 0.5×10^6 cells/ml in a 96-well plate in X-Vivo complete medium, with and without IL-2 (600 IU/ml). Supernatants were then collected at 24 h.

Cytotoxicity assays. $CD56^+CD3^-CD19^-CD14^-$ cells from slowly growing TIL cultures that suppressed TILs in functional assays (regulatory $CD56^+CD3^-$ cells) and $CD56^+CD3^-CD19^-CD14^-$ cells from the peripheral blood of healthy donors (PB NK cells) were isolated by flow cytometry–based sorting and co-cultured with K562 cells (ATCC) in the presence of IL-2. These cells were not tested for mycoplasma. The percentage of CD107a expression by $CD56^+CD3^-$ cells and the fold increase in expression of fixable viability dye (eBioscience) by K562 cells were analyzed after 6 h.

Analysis of publically available microarray data. *NCAM1* (CD56) gene expression from the Tothill data set of 215 patients with HGSC[34] was ranked from high to low, and Kaplan–Meier curves were generated using the corresponding overall survival and recurrence-free survival data (CD56 high, $n = 107$; CD56 low, $n = 107$). The caveats of using CD56 as a marker, however, include that ~5% of the HGSC tumors we examined by IHC were $CD56^+$ and non-$CD56^+$ ILCs are not captured with this marker.

Statistical analysis. Statistical significance was determined by two-tailed Mann–Whitney test or Wilcoxon matched-pairs signed-rank test. For Kaplan–Meier curves, significance was determined by log-rank (Mantel–Cox) test. The n values used to calculate statistics are defined and indicated in figure legends. Significance is indicated within figures, and if differences were not significant ($P > 0.05$) this is denoted by n.s.

Data availability. The RNA–seq data set generated during the current study is not publicly available, as this would compromise research participant privacy/consent. The data that support the findings of this study are available from the corresponding author upon reasonable request.

42. Dobin, A. *et al.* STAR: ultrafast universal RNA–seq aligner. *Bioinformatics* **29**, 15–21 (2013).
43. DeLuca, D.S. *et al.* RNA-SeQC: RNA–seq metrics for quality control and process optimization. *Bioinformatics* **28**, 1530–1532 (2012).
44. Li, B. & Dewey, C.N. RSEM: accurate transcript quantification from RNA–Seq data with or without a reference genome. *BMC Bioinformatics* **12**, 323 (2011).
45. Love, M.I., Huber, W. & Anders, S. Moderated estimation of fold change and dispersion for RNA–seq data with DESeq2. *Genome Biol.* **15**, 550 (2014).

doi:10.1038/nm.4278